Synthesis, aqueous solution behavior and self-assembly of a dual pH/thermo-responsive fluorinated diblock terpolymer

Panagiotis Falireas, Vincent Ladmiral, Bruno Ameduri

Synthesis, aqueous solution behavior and self-assembly of a dual pH/thermo-responsive fluorinated diblock terpolymer

Panagiotis G. Falireas, Vincent Ladmiral, and Bruno Ameduri**

ICGM, Univ Montpellier, CNRS, ENSCM, Montpellier, France.

*Corresponding Authors: E-mail: bruno.ameduri@enscm.fr (B. Améduri)

E-mail: pfalireas@uliege.be (P. Falireas)

ABSTRACT

The synthesis of fluorinated dual-responsive block terpolymers via sequential reversible addition-fragmentation chain transfer (RAFT) polymerization is presented. The resulting block terpolymers consist of a hydrophobic block which comprises an alternating copolymer of *tert*-butyl-2-trifluoromethacrylate (MAF-TBE) and vinyl acetate (VAc) (M_n = 9,800 g/mol, $Đ$=1.31) and a hydrophilic block of temperature-responsive poly(*N*-isopropylacrylamide) (PNIPAM). Two P(VAc-*alt*-MAF-TBE)-*b*-PNIPAM block terpolymers, containing 37 and 61 mol % of NIPAM, (with M_n = 16,600 g/mol, $Đ$=1.13 and M_n = 22,400 g/mol, $Đ$=1.28, respectively) were synthesized in good yelds. Subsequent hydrolysis of the ester groups in the P(MAF-TBE-*alt*-VAc) segments resulted in the formation of a double hydrophilic pH and temperature-responsive diblock terpolymers which demonstrated remarkable solution properties. The impact of the trifluoromethyl groups on the aqueous solution behavior of the diblock terpolymers was studied by monitoring the lower critical solution temperature (LCST) using UV/vis spectroscopy at different pH values (ranging from 9.5 to 2.5). This study revealed that the fluorinated moieties dictate the solvation of the terpolymers inducing attractive hydrophobic interactions which drove the system to phase separation. Additionally, other amphiphilic diblock terpolymers were prepared by extension of the P(VAc-*alt*-MAF-TBE) macromolecular chain transfer agent with hydrophilic poly(*N*,*N*-dimethylacrylamide) (PDMA) (M_n =14,000 g/mol, $Đ$=1.21 for 52 mol% PDMA and M_n =19,000 g/mol, $Đ$=1.45 for 79 mol% PDMA). Transmission electron microscopy measurements showed that the diblock terpolymers can self-assemble in aqueous solution to form various micellar or vesicular morphologies depending on the terpolymer composition and solution pH, rendering them attractive for drug delivery and in other biomedical applications.

Introduction

The field of stimuli-responsive polymers have been established and extensively developed in the past two to three decades.[1] These elegant materials differ from common polymers with their ability to respond to certain changes in their microenvironment by adjusting their physical and/or chemical properties. In particular, stimuli-responsive polymers have been designed and synthesized to be responsive to a variety of external stimuli such as pH,[2, 3] temperature,[4, 5] light,[6, 7] ionic strength,[8, 9] or mechanical force or stress.[10, 11] The receptor of the stimulus is usually a

pendant functional group located along the polymer chain able to respond to a single or multiple stimuli.[12-14] The advancement of polymer chemistry gave an impetus towards the preparation of such materials leading to a significant increase of the number of research articles in this field over the last decades. Besides the synthesis of these niche polymers, the study of their properties and by extension of the applications that can emerge have also attracted a great interest.[1] Stimuli-responsive (co)polymers have found a plethora of applications such as drug delivery carriers,[15, 16] sensors,[17, 18] biosensors,[19] stabilization of colloidal dispersions, etc.[20, 21]

Fluorine-containing (co)polymers constitute a unique class of high-performance materials endowed with outstanding properties which emerge from the electronic structure of fluorine atoms. More precisely, the small van del Waals radius, high electronegativity and low polarizability of fluorine atom as well as the strongly polarized C-F bond that induces a strong and short bond (~490 KJ mol^{-1}). This chemistry endow fluorinated polymers with extraordinary thermal and chemical stabilities rendering them attractive for many applications.[22-28] Specially, due to the bioinertness, low surface energy as well as their low solubility in water, which promotes self-aggregation, fluoropolymers are widely used in several biological and medical materials [29, 30] such as drug and gene delivery,[31-33] dental implants,[34] anti-fouling coatings,[35, 36] blood substitutes[37] and contact lenses[38].

In recent years, the incorporation of fluorinated groups or sequences into functional copolymers led to the preparation of stimuli-responsive fluorinated block polymers exhibiting pH,[39, 40] thermo,[41-44] and light [45] responsive features. However, reports on the synthesis and systematic investigation of the properties of fluorine containing-(co)polymers able to respond to multiple stimuli is still a challenging task. Liu et al. described the preparation of dual responsive fluorinated diblock copolymers via oxyanion-initiated polymerization.[46] The resulting block copolymers consisted of a dual-responsive hydrophilic block of poly[2-(dimethylamino)ethyl methacrylate] (PDMAEMA) and a hydrophobic block of poly(2, 2, 2-trifluoroethyl methacrylate) (PTFMA). The solution behaviors of these copolymers were studied by DLS and UV measurements. The results indicated that these fluorinated diblock copolymers possess distinct pH/temperature-responsive properties, depending not only on the PDMA segment but also on the fluoroalkyl structure of the fluoroalkyl methacrylate units.

Driven by the attractive properties of stimuli responsive fluoropolymers, we explored the preparation via RAFT polymerization of a new pH/temperature dual-responsive fluorinated

diblock terpolymer. This diblock terpolymer consists of an alternating block of *tert*-butyl-2-trifluoromethacrylate (MAF-TBE) and vinyl acetate (VAc) chain extended with poly(*N*-isopropylacrylamide) (NIPAM). The simultaneous hydrolysis of the *tert*-butyl ester and acetate groups of the MAF-TBE and VAc, respectively, led to the formation of double hydrophilic diblock terpolymers able to respond to both pH and temperature. The effect of varying the relative block compositions under the cooperative combined effects of pH and temperature on the phase transition of the resulting responsive materials was investigated. In addition, similar amphiphilic diblock terpolymers of different block lengths were formed by the chain extension of the P(VAc-*alt*-MAF-TBE) macroCTA with hydrophilic poly(*N*,*N*-dimethylacrylamide), PDMA.[47] All the synthesized terpolymers were thoroughly characterized and the relationship of their structure with their self-assembly behavior was examined.

Experimental Section

Materials and methods

Tert-butyl-2-trifluoromethacrylate (MAF-TBE) was kindly offered by Tosoh Fine Chemical Corporation, Shunan, Japan. Cyanomethyl 3,5-dimethyl-1H-pyrazole-1-carbodithioate (CDPCD) was synthesized according to the method described by Gardiner et al.[48] 2,2-azobis (4-methoxy-2,4-dimethylvaleronitrile) (V-70, Wako), *N*,*N*-dimethylacrylamide (DMA, 99%, Aldrich), *N*-isopropylacrylamide (NIPAM, Aldrich, ≥99%), vinyl acetate (VAc, Aldrich, ≥99%), potassium hydroxide, (KOH, Aldrich, ≥85%), acetone (Aldrich, ≥99.5%), ethanol (Aldrich, ≥99.9%),) dimethylformamide (DMF, Aldrich, 99.8%) were used as received. Milli-Q water of specific resistivity of 18.2 MΩ cm at 25 °C was used in all experiments. Deuterated solvents used for ^{1}H, ^{13}C and ^{19}F nuclear magnetic resonance (NMR) spectroscopy was purchased from Euroisotop (Saint-Aubin, France). Any glassware was cleaned in a KOH/isopropanol bath and dried under vacuum prior to use.

Synthesis of P(VAc-*alt*-MAF-TBE) macroCTA

The P(VAc-*alt*-MAF-TBE) RAFT macroCTA was synthesized using a procedure similar to that described previously.[49] A typical procedure (Scheme 1-a) is described below: MAF-TBE (12.51 g, 63.70 mmol), VAc (5.49 g, 63.70 mmol), CDPCD (0.50 g, 2.70 mmol) and V-70

(73.00 mg, 0.20 mmol) were added in a 100 ml round bottom flask equipped with a magnetic stirrer under a nitrogen flow. Subsequently, the flask was sealed with a rubber septum and the reaction mixture was stirred for 20 min at ambient temperature. Then, the yellowish mixture was degassed by three freeze-pump-thaw cycles and the reaction was allowed to proceed at 40 ^{o}C until almost complete monomer consumption. After completion of the polymerization, a sample from the reaction mixture was removed for ^{1}H and ^{19}F NMR analysis where VAc and MAF-TBE conversions were determined (monomer conversions = 90 %). The polymerization was terminated by immersing the flask in liquid nitrogen and opening it to air. Subsequently, the copolymer was dissolved in acetone, precipitated twice from chilled water and isolated by filtration. Finally, the purified copolymer (yellowish crystals) was dried under vacuum for 24 h at 60 ^{o}C (15.8 g, yield=85 %), and characterized by ^{1}H, ^{13}C and ^{19}F NMR spectroscopies and gel permeation chromatography (GPC) (M_n = 9,800 g/mol, $Đ$=1.31, Table 1).

^{1}H NMR (400 MHz, $CDCl_3$, δ (ppm), Figure S1 a): 1.49 (s, 9H, -C(C$\underline{H}_3$)$_3$), 1.99 (s, 3H, -C$\underline{H}_3$), 2.05-2.42 (m, 4H, -C$\underline{H}_2$- of VAc and MAF-TBE), 5.24 (m, 1H, -C$\underline{H}$OAc). ^{13}C NMR (101 MHz, $CDCl_3$, δ (ppm), Figure 2a): 21.07 (-$\underline{C}H_3$), 27.73 (-C($\underline{C}H_3$)$_3$), 35.70-40.01 (-$\underline{C}H_2$- of VAc and MAF-TBE), 53.75 (q, $^{2}J_{C\text{-}F}$=30 Hz, -$\underline{C}$-CF$_3$), 65.00-68.83 (-$\underline{C}$HOAc), 83.22 (-$\underline{C}$(CH$_3$)$_3$), 120.66-131.11 (q, $^{1}J_{C\text{-}F}$=280 Hz, -$\underline{C}F_3$), 167.06 (-O-($\underline{C}$=O)CH$_3$), 169.09 (-($\underline{C}$=O)-O-C(CH$_3$)$_3$). ^{19}F NMR (377 MHz, $CDCl_3$, δ (ppm), Figure S2): -67.66 (-C$\underline{F}_3$).

Synthesis of P(VAc-*alt*-MAF-TBE)-*b*-PDMA and P(VAc-*alt*-MAF-TBE)-*b*-PNIPAM diblock terpolymers

The synthesis of the P(VAc-*alt*-MAF-TBE)-*b*-PDMA diblock terpolymers was conducted using the above-synthesized P(VAc-*alt*-MAF-TBE) macroCTA for the polymerization of DMA (Scheme 1-c). In a 100 mL dried round bottom flask equipped with a magnetic stirrer, P(VAc-*alt*-MAF-TBE) macroCTA (0.611 g), V-70 (3.80 mg, 0.012 mmol), DMA (1.45 ml, 12 mmol) and DMF (12 ml) were transferred under a nitrogen flow. The reaction mixture was stirred for 20 min at ambient temperature and deoxygenated by three freeze-pump-thaw cycles and the flask was placed in a preheated oil bath at 40 ^{o}C for 6 h. The polymerization was terminated by immersing the flask into liquid nitrogen and opening it to air. An aliquot was removed for ^{1}H NMR analysis (DMA conversion = 95 %). The polymer solution was dried under vacuum at 60 ^{o}C for 24 h. It was then dissolved in acetone and precipitated twice from chilled hexane. The

purified product (yellowish crystals) was then dried under vacuum at 60 °C for 24 h (1.75 g, yield=88%). The terpolymer was characterized by ^{1}H NMR spectroscopy for the determination of the molar composition and by GPC for the estimation of molar masses. Two diblock terpolymers with different compositions and molar masses were synthesized by varying the $[DMA]_o$: $[P(VAc\text{-}alt\text{-}MAF\text{-}TBE)\ macroCTA]_o$ molar ratio (Table 1). This polymerization procedure yielded a P(VAc-*alt*-MAF-TBE)-*b*-PDMA diblock terpolymer containing 52 mol % PDMA, with M_n = 14,100 g/mol and $Đ$ = 1.21. Using the same procedure, another diblock terpolymer, P(VAc-*alt*-MAF-TBE)-*b*-PDMA block terpolymer, containing a higher PDMA molar composition (79 mol % PDMA), with M_n = 19,000 g/mol and $Đ$ = 1.45 (Table 1) was synthesized. In the following, the diblock terpolymers with PDMA contents of 52 and 79 mol % will be referred as P(VAc-*alt*-MAF-TBE)-*b*-PDMA-1 and P(VAc-*alt*-MAF-TBE)-*b*-PDMA-2, respectively.

^{1}H NMR (400 MHz, $CDCl_3$, δ (ppm), Figure 5a): 1.42 (s, 9H, -C($C\underline{H}_3$)$_3$), 1.56-2.30 (m, 6H, -$C\underline{H}_2$- of VAc, MAF-TBE and DMA), 1.91 (s, 3H, -$C\underline{H}_3$), 2.59 (s, 1H, -$C\underline{H}$- of DMA), 2.85 (s, 6H -N($C\underline{H}_3$)$_2$, 5.15 (m, 1H, -$C\underline{H}$OAc).^{13}C NMR (101 MHz, $CDCl_3$, δ (ppm), Figure S3): 21.15 (-$\underline{C}H_3$), 27.69 (-C($\underline{C}H_3$)$_3$), 33.90-39.63 (-N($\underline{C}H_3$)), (-$\underline{C}$H-), and -($\underline{C}H_2$-) of DMA, -$\underline{C}H_2$- of VAc and MAF-TBE, 54.00 (q, $^2J_{C\text{-}F}$=30 Hz, -$\underline{C}$-CF_3), 66.20 (-$\underline{C}$H- of VAc), 83.27 (-C($\underline{C}H_3$)$_3$), 120.66-131.11 (q, $^1J_{C\text{-}F}$=280 Hz, -$\underline{C}F_3$), 162.55 (-O-($\underline{C}$=O)CH_3), 167.06 -($\underline{C}$=O)-N$(CH_3)_2$, 169.81 (-($\underline{C}$=O)-O-C$(CH_3)_3$).^{19}F NMR (377 MHz, $CDCl_3$, δ (ppm), Figure S4): 67.68.

The same experimental procedure was followed for the synthesis of P(VAc-*alt*-MAF-TBE)-*b*-PNIPAM diblock terpolymers (Scheme 1-d). As for the PDMA diblock terpolymer described above, two different diblock terpolymers containing different PNIPAM molar ratios were synthesized. The purified polymers (yellowish crystals) were characterized by ^{1}H NMR spectroscopy and GPC: P(VAc-*alt*-MAF-TBE)-*b*-PNIPAM-1 composed of 37 mol % of PNIPAM, with M_n = 16,600 g/mol and $Đ$ = 1.13 (yield=70 %); and P(VAc-*alt*-MAF-TBE)-*b*-PNIPAM-2 containing 61 mol% of PNIPAM (M_n = 22,400 g/mol and $Đ$ = 1.28; yield=76 %) (Table 1).

^{1}H NMR (400 MHz, $CDCl_3$, δ (ppm), Figure 5b): 1.13 (s, 6H, (-$C\underline{H}_3$)$_2$), 1.46 (s, 9H, (-$C\underline{H}_3$)$_3$), 1.95 (s, 3H, (-$C\underline{H}_3$), 1.5-2.4 (m, 6H, -$C\underline{H}_2$- of MAF-TBE, VAc and NIPAM), 3.99 (s, 1H, (-$C\underline{H}(CH_3)_2$), 5.20 (m, 1H,-$C\underline{H}$OAc), 5.42 (s, -N-$\underline{H}$). ^{13}C NMR (101 MHz, $CDCl_3$, δ (ppm), Figure 6a): 21.04 (-$\underline{C}H_3$), 22.69 (-CH($\underline{C}H_3$)$_2$), 27.73 (-$\underline{C}$(CH_3)$_3$), 33.10-39.10 (-$\underline{C}H_2$- of NIPAM, VAc

and MAF-TBE), 42.60 (-CH(CH_3), 53.96 (q, $^2J_{C-F}$=30 Hz, -C-CF_3), 66.31 (-CHOAc), 83.55 (-C(CH_3)$_3$), 120.66-131.11 (q, $^1J_{C-F}$=280 Hz, -CF_3), 167.06 (-O-(C=O)CH_3), 169.63 (-(C=O)-O-C(CH_3)$_3$), 174.01 ((-C=O)-NH-). ^{19}F NMR (377 MHz, $CDCl_3$, Figure S5) δ (ppm): 67.72.

Hydrolysis of *tert*-butyl ester and acetate groups of P(VAc-*alt*-MAF-TBE) copolymer

Briefly, P(VAc-*alt*-MAF-TBE) (2.02 g), ethanol (10 mL) and a solution of potassium hydroxide (7 g KOH in 45 mL of water) were transferred into a 100 ml flask equipped with a reflux condenser. The polymer solution was then stirred and heated at 60 ^oC for 48 h. In the initial stages of the hydrolysis, the copolymer remained insoluble. As the reaction proceeded, the copolymer slowly dissolved in the reaction medium. Then, the aqueous solution of the copolymer was dialyzed against water for 72 h (the water was replaced every 6 h to remove excess KOH and fragments resulting from hydrolysis). Then, the purified copolymer was isolated after lyophilization as white crystals. The successful cleavage of the ester functions was confirmed by ^{1}H, ^{13}C and ^{19}F NMR spectroscopies. This hydrolyzed copolymer is referred to as P(VOH-*alt*-MAF) copolymer.

^{1}H NMR (400 MHz, D_2O, δ (ppm), Figure S1 b):1.60-2.40 (m, 4H, -CH_2- of VOH and MAF), 4.01(m, 1H, -CHOAc). ^{13}C NMR (101 MHz, D_2O, δ (ppm), Figure 2b): 35.8-45.4 (-CH_2- of VOH and MAF), 54.74 (q, $^2J_{C-F}$=30 Hz, -C-CF_3), 62.17-66.53 (-CH-OH), 121.48-133.03 (q, $^1J_{C-F}$=280 Hz, -CF_3), 176.16 (-(C=O)-OH). ^{19}F NMR (377 MHz, D_2O, δ (ppm), Figure S6): 68.66-66.86 (-CF_3).

The same conditions were used for the hydrolysis of P(VAc-*alt*-MAF-TBE)-*b*-PNIPAM-1 into P(VOH-*alt*-MAF)-*b*-PNIPAM block copolymer (Scheme 1-e).

^{1}H NMR (400 MHz, D_2O, δ (ppm), Figure S7):1.09 (s, 6H, (-CH_3)$_2$), 1.27-2.29 (m, 7H, -CH_2- of MAF-TBE, VAc and NIPAM, -CH- of NIPAM), 3.83 (s, 1H, -CH(CH_3)$_3$), 4.03 (m, 1H, -CHOAc). ^{13}C NMR (101 MHz, D_2O, δ (ppm) Figure 6b): 21.53 (-CH_3), 38.40-45.65 (-CH_2- of NIPAM, VOH and MAF), 54.70 (q, $^1J_{C-F}$=30 Hz, -C-CF_3), 65.18 (-CH-OH), 121.82-134.45 (q, $^2J_{C-F}$=280 Hz, -CF_3), 175.9 ((-C=O)-NH-) and (-(C=O)-OH). ^{19}F NMR (377 MHz, D_2O, δ (ppm) Figure S8): 67.68 -CF_3.

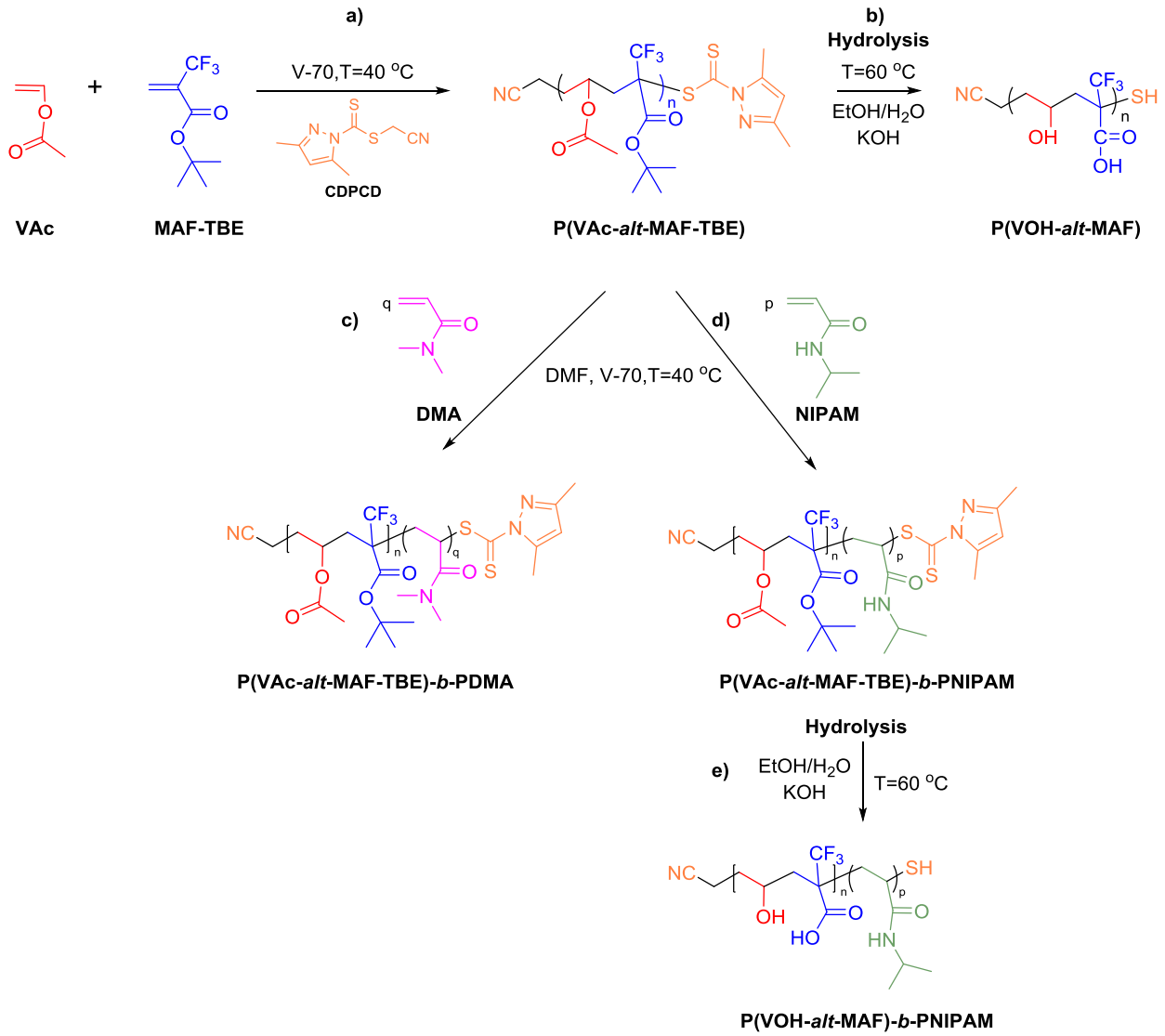

Scheme 1. Synthesis routes of the diblock terpolymers: a) synthesis of P(VAc-*alt*-MAF-TBE) macroCTA; b) hydrolysis of P(VAc-*alt*-MAF-TBE) to P(VOH-*alt*-MAF); c) synthesis of P(VAc-*alt*-MAF-TBE)-*b*-PDMA, d) synthesis of P(VAc-*alt*-MAF-TBE)-*b*-PNIPAM, e) hydrolysis of P(VAc-*alt*-MAF-TBE)-*b*-PNIPAM into P(VOH-*alt*-MAF)-*b*-PNIPAM.

Self-assembly of the P(VAc-*alt*-MAF-TBE)-*b*-PDMA and P(VAc-*alt*-MAF-TBE)-*b*-PNIPAM diblock terpolymers

To study the self-assembly of diblock terpolymers in aqueous solution, polymer solutions were prepared by dissolving 10 mg of terpolymer in 2 mL of acetone, a good solvent for both blocks. Under vigorous stirring, 8 mL of deionized water (pH=7.0, 25 °C) were added dropwise to each

of these acetone solutions, and the resulting mixtures were stirred slowly for 12 h. Next, the solutions were dialyzed against deionized water using a dialysis membrane (MWCO 3,000 Da) for 24 h, to remove the acetone (the water was replaced every 6 h). The same procedure was followed for the P(VOH-*alt*-MAF-TBE)-*b*-PNIPAM diblock terpolymers. The pH solution was adjusted by the manual addition of HCl or NaOH aliquots of 0.1 M.

Characterizations

Nuclear Magnetic Resonance (NMR) Spectroscopy

The microstructures of the terpolymers were determined by ^{1}H, ^{13}C and ^{19}F NMR spectroscopies, recorded on a Bruker AC 400 Spectrometer (400 MHz for ^{1}H, 101 MHz for ^{13}C and 376 MHz for ^{19}F). Coupling constants and chemical shifts are given in Hertz (Hz) and parts per million (ppm), respectively. The experimental conditions for recording ^{1}H [or ^{13}C or ^{19}F] NMR spectra were as follows: flip angle 90 ° [or 90 °or 30 °], acquisition time 4.5 s [or 0.3 s or 0.7 s], pulse delay 2 s [or 1 or 5 s], number of scans 32 [or 8192 or 64], and a pulse width of 12.5, 9.5 and 5.0 μs for ^{1}H, ^{13}C and ^{19}F NMR, respectively.

Gel permeation chromatography (GPC)

The apparent number average molar masses and dispersities of the synthesized polymers were determined using a GPC system (Varian 390-LC) multi-detector equipped with a differential refractive index detector (RI), using a guard column (Varian Polymer Laboratories PLGel 5μm, 50 x 7.5 mm), and two ResiPore columns of the same type. The mobile phase was DMF with 0.1 wt % LiBr adjusted at a flow rate of 1 mL min^{-1} while the columns were thermostated at 70 ^{o}C. The GPC system was calibrated using narrow poly(methyl methacrylate) (PMMA) standards ranging from 550 to 1,568,000 g/mol (EasiVial-Agilent).

Potentiometric titration

The potentiometric titration of the P(VOH-*alt*-MAF) alternating copolymer was conducted using a Thermo Scientific Orion (RL150) pH-meter which was calibrated at pH 4, 7 and 10 using buffer solutions. Initially, 0.10 g of terpolymer was dissolved in 100 mL of Milli-Q water and, upon stirring, aliquots of 1M NaOH were added until the pH of the polymer solutions reached

pH 10. The titration curves were obtained by monitoring the decrease of the solution pH upon addition of aliquots of 0.1 M HCl up to pH 2. The pH value was adjusted after the addition of every aliquot and the pH was registered after stabilization.

Zeta Potential measurements

Aqueous electrophoretic measurements of the polymer aqueous solutions (0.01 wt%) as a function of pH were conducted using a Malvern Zetasizer NanoZS instrument. Measurements were carried out in the presence of 0.1 mM KCl background electrolyte. The pH of the solution was adjusted by adding 0.1 M NaOH or HCl aqueous solutions. Three measurements were recorded for each sample and the zeta potential was calculated from the electrophoretic mobility using the Smoluchowski equation.

Transmission electron microscopy (TEM)

TEM was performed on a Jeol 1200EXII transmission electron microscope at an operating voltage of 100 kV with images captured by means of a Quemesa camera from Olympus Soft Imaging Solutions. Terpolymer solutions in pH 9.5 and 3.5 solutions were prepared using the procedure described above and allowed to stand at 25 ^{o}C for 4 h prior to TEM sample preparation. One drop of polymer solutions (0.1 wt%) was placed onto a Formvar-coated, 300-mesh copper grid, stabilized with evaporated carbon film for TEM analysis and left to dry under air prior to analysis. The average size of the produced aggregates was assessed using ImageJ.

UV/vis spectroscopy

The thermosensitivity of 1 wt % P(VOH-*alt*-MAF)-*b*-PNIPAM diblock terpolymers was measured on a Cary 50 Varian UV/vis spectrophotometer equipped with a temperature-controlled sample holder. The polymer solution was prepared by dissolving the terpolymer in aqueous solution (pH=10, 25 ^{o}C) and the pH was adjusted by adding aliquots of 0.1 M HCl. The transmittance of the terpolymer solution was monitored in a quartz cuvette at a detection wavelength of 500 nm at a heating rate of 10 °C/min from 25 to 80 °C at different pH values.

Fourier transform infrared spectroscopy (FTIR)

FTIR analyses of the polymer were performed using a PerkinElmer Spectrum 1000 in ATR mode, with an accuracy of ±2 cm^{-1}.

Dynamic light scattering (DLS)

The average hydrodynamic diameter (D_h) of P(VOH-*alt*-MAF)-*b*-PNIPAM diblock terpolymers self-assembled structures was determined as a function of solution pH using a Delsa Nano C, Particle Analyzer, Beckman Coulter at 25 °C and the intensity of scattered light was detected at 165° to the incident beam. The reported values are the intensity-average hydrodynamic diameters. Each measurement was repeated 3 times.

Results and Discussion

Synthesis of P(VAc-*alt*-MAF-TBE) macroCTA

The P(VAc-*alt*-MAF-TBE) macroCTA was synthesized using a procedure similar to that described in a previous article.[49] MAF-TBE is a fluorinated monomer which has been studied for specific materials in lithium ion batteries, fuel cell membranes and photoresist lithography.[50-54] A main characteristic of alkyl 2-trifluoromethyl acrylates (and hence of MAF-TBE) is that they do not homopolymerize under radical conditions,[55, 56] while anionic polymerization is successful.[57, 58] Therefore, MAF-TBE has only been copolymerized by radical polymerization with various monomers (fluorinated or non-fluorinated).[54, 59-62] VAc was chosen as a comonomer as its copolymerization with MAF-TBE was shown to result in perfectly alternating copolymers. This alternating structure is due to the high electron-donating character of VAc whereas MAF-TBE is an electron-accepting species.[63, 64] The copolymerization was performed using CDPCD as a chain transfer agent using 2,2-azobis (4-methoxy-2,4-dimethylvaleronitrile) (V-70) as the thermal initiator at 40 ^{o}C (Scheme 1-a). The resulting copolymer showed low dispersity ($Đ$=1.31) suggesting a possible controlled copolymerization. The formation of an alternating copolymer was verified by ^{1}H NMR spectroscopy (Figure S1 a). Characteristic signals of both comonomer units were observed. Nevertheless, signals attributed to CDPCD were not clearly identified. Therefore, the calculation of the molar masses using ^{1}H NMR was not appropriate.

The $[VAc]_o$:$[MAF\text{-}TBE]_o$ molar ratio was determined by comparing the peak integrals of the strong singlet at 1.49 ppm assigned to methyl groups in MAF-TBE segments and the peak centered at 5.24 ppm corresponding to -C<u>H</u>OAc of VAc. This ratio was found to be 49:51 thus confirming the alternating microstructure. The ^{19}F NMR spectrum of the alternating copolymer (Figure S2) presents the characteristic signal at -67.66 ppm of $-CF_3$ group in MAF-TBE units of the copolymer.

Table 1. Molecular characteristics of P(VAc-*alt*-MAF-TBE)-*b*-DMA and P(VAc-alt-MAF-TBE)-*b*-PNIPAM diblock terpolymers derived from P(VAc-*alt*-MAF-TBE) macroCTA via sequential RAFT copolymerization.

Entry	Sample	M_n[a] (g/mol)	$Đ$[a]	$F_{MAF\text{-}TBE}$[b] (% mol)	F_{VAc}[b] (% mol)	$F_{PDMA\ or\ PNIPAM}$[b] (% mol)
1	P(VAc-*alt*-MAF-TBE)	9,800	1.31	51	49	0
2	P(VAc-*alt*-MAF-TBE)-*b*-PDMA-1	14,100	1.21	25	23	52
3	P(VAc-*alt*-MAF-TBE)-*b*-PDMA-2	19,000	1.45	11	10	79
4	P(VAc-*alt*-MAF-TBE)-*b*-PNIPAM-1	16,600	1.13	32	31	37
5	P(VAc-*alt*-MAF-TBE)-*b*-PNIPAM-2	22,400	1.28	19	20	61

[a] Number average molar mass and dispersity of the terpolymers measured by GPC relative to poly(methyl methacrylate) standards in DMF at 40 ^oC, [b] Determined by ^1H NMR.

Hydrolysis of *tert*-butyl ester and acetate groups of P(VAc-*alt*-MAF-TBE) and study of aqueous solution properties of P(VOH-*alt*-MAF) copolymer

The P(VAc-*alt*-MAF-TBE) copolymer before hydrolysis was highly hydrophobic. Therefore, to alter the hydration state, the simultaneous cleavage of all ester groups in both VAc and MAF-

TBE units was achieved. The hydrolysis was performed using aqueous alkaline solution following conditions previously reported (Scheme 1-b).[65]

FTIR spectra of P(VAc-*alt*-MAF-TBE) and P(VOH-*alt*-MAF) were acquired to confirm the success of hydrolysis (Figure 1). The presence of the *tert*-butyl ester groups of the P(VAc-*alt*-MAF-TBE) copolymer was evidenced in the IR spectrum (Figure 1a) by the bands at 2934, 2986 cm^{-1} and 1368 cm^{-1} which were assigned to the asymmetric stretching and bending of C-H of CH_3 groups. The frequency at 1231 cm^{-1} is assigned to C-O-C groups of VAc while the peak at 1736 cm^{-1} was assigned to the stretching of the carbonyl of the ester groups in both MAF-TBE and VAc.[66, 67] The characteristic absorption of CF_3 group is observed at 1084 cm^{-1}. After hydrolysis, the *tert*-butyl groups of MAF-TBE and the methyl end groups of the acetate of VAc were converted into carboxylic acid and alcohol, respectively. This was evidenced by a broad stretch observed at 3100-3500 cm^{-1} due to the formation of hydroxyl groups, and the vanishing of the peak at 1368 cm^{-1} assigned to the methyl groups as well as at 1231 cm^{-1} due to C-O-C of VAc. Moreover, the C=O absorption peak at 1736 cm^{-1} disappeared and two new peaks appeared at 1773 cm^{-1} and 1592 cm^{-1}. These results are in agreement with the previously reported hydrolysis of *tert*-butyl ester of poly(VDF-*co*-MAF-TBE) copolymers to prepare -COOH functionalized PVDF.[61]

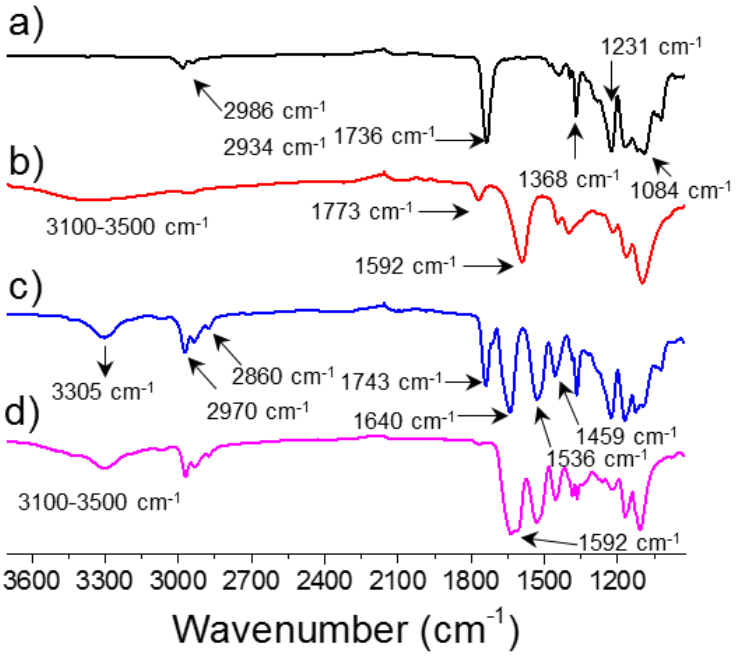

Figure 1. Typical FT-IR spectra of a) P(VAc-*alt*-MAF-TBE), b) P(VOH-*alt*-MAF), c) P(VAc-*alt*-MAF-TBE)-*b*-PNIPAM-2, d) P(VOH-*alt*-MAF)-*b*-PNIPAM-2 copolymers. the spectra were recorded on powder using an ATR module

^{1}H and ^{13}C NMR spectra provided additional evidence of the concomitant hydrolysis of both ester groups. Figure 2a represents the fully assigned ^{13}C NMR spectrum of P(VAc-*alt*-MAF-TBE) macroCTA. The characteristic signals at 27.73 and 83.22 ppm of the *tert*-butyl groups of MAF-TBE as well as the methyl end group of acetate at 21.04 ppm and the carbonyl group at 167.06 ppm of VAc have completely disappeared after hydrolysis (Figure 2b). ^{1}H NMR spectroscopy also confirmed the hydrolysis of the ester groups. The signal corresponding to the CH group in the VAc units in the alternating dyad (signal 2, in Figure S1 b) was shifted toward lower fields by about 1.20 ppm as reported in previous studies.[68] Moreover, the sharp peaks of resonances assigned to the *tert*-butyl group of MAF-TBE at 1.49 ppm and CH_3 groups of VAc at 1.99 ppm entirely disappeared. These results also demonstrate the complete hydrolysis of the ester groups.

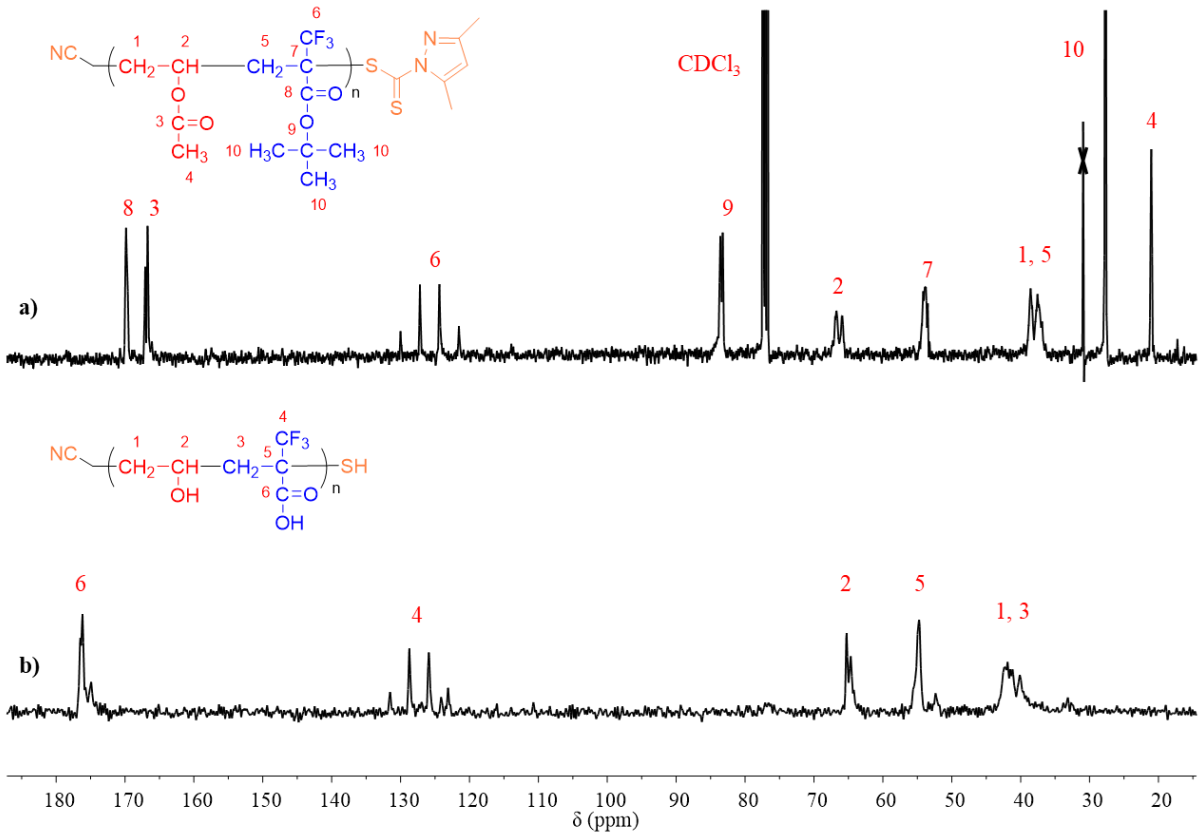

Figure 2. ^{13}C NMR spectra of: a) P(VAc-*alt*-MAF-TBE), and b) P(VOH-*alt*-MAF) copolymers recorded in $CDCl_3$ and D_2O, respectively. The crossed-out signal is solvent (acetone, 31.05 ppm).

The successful hydrolysis of the ester groups promoted the solubility in water of the resulting copolymer containing hydrophilic alcohol and pH-responsive trifluoromethacrylic acid moieties. Only a few reports deal with the pH-dependent behavior of poly(trifluoromethacrylic acid).[69, 70] The CF_3 group, which is considered as an electron-withdrawing substituent, is known to render MAF as a relatively strong acid. The acid dissociation constant (pK_a) of MAF was experimentally calculated as 2.7 ± 0.1 by potentiometric titrations and 2.1 ± 0.2 by simulation studies.[69, 70] Another study showed that copolymerization of MAF with ethylene glycol dimethacrylate resulted in a significant increase of pK_a at 5.7 ± 0.1.[69] In the present case, each MAF unit is adjacent to two hydrophilic vinyl alcohol units which in turn might also alter the pK_a of the copolymer. Therefore, to examine the responsive properties of this copolymer in aqueous media, the effect of the solution pH on the ionization behavior of P(VOH-*alt*-MAF) was studied by means of *in situ* potentiometric titration and zeta potential measurements.

The titration curve of the P(VOH-*alt*-MAF) copolymer is shown by Figure 3a where the abscissa axis represents the net amount of HCl added. Starting from basic conditions, the sharp decrease of the pH from 10 to 6 is attributed to the neutralization of NaOH by HCl. From pH 5.5, the onset of a plateau regime is discerned due to the protonation of MAF units in the copolymer. However, as pH was further reduced (pH < 3), the copolymer solution became turbid inducing a precipitation (Figure 3a, inset). This behavior did not permit the complete protonation of the carboxylate groups as no inflection points were observed. Consequently, the experimental determination of the pK_a value of the copolymer was not possible. Nevertheless, it is speculated that the pK_a should be located in solution regime below pH=3, in line with previous experimental and theoretical studies.[69, 70]

To gain further insight into the aqueous solution properties of this alternating copolymer, the evolution of the zeta potential as a function of pH was also recorded (Figure 3b).

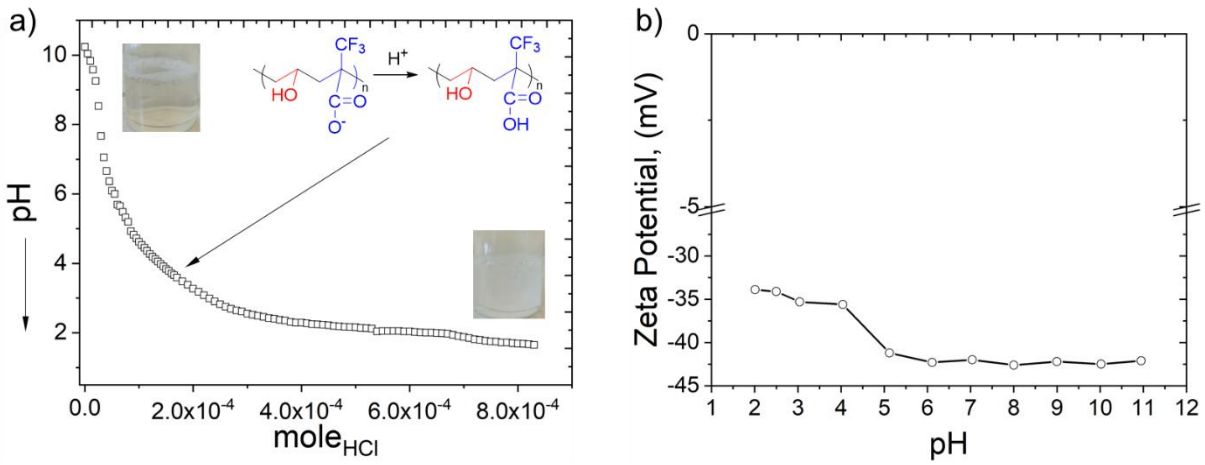

Figure 3. a) Titration curve and b) zeta potential of the P(VOH-*alt*-MAF) copolymer as a function of solution pH.

The zeta potential-pH profile shows highly negative values over the whole pH regime tested (from 11 to 2) which is attributed to the negatively charged carboxylate groups of MAF units. In particular, from pH 11 to 5, constant negative values were recorded, while for pH below 5 the observed slight increase of the charge could be explained by the protonation of a portion of the carboxylates. At this pH regime, the copolymer solution became turbid suggesting the formation of aggregates which in turn impaired the completion of the protonation of MAF units as in the titration measurements. Both experiments lead to the conclusion that the formation of aggregates in acidic media was attributed to two synergetic effects: 1) the protonation of the carboxylate groups, which deter the polymer chains to expand via charge repulsion, and 2) the unfavorable hydrophobic interactions caused by the -CF_3 groups

Syntheses of P(VAc-*alt*-MAF-TBE)-*b*-PDMA and P(VAc-*alt*-MAF-TBE)-*b*-PNIPAM block copolymers by chain extension from P(VAc-*alt*-MAF-TBE) macroCTA

The ability of P(VAc-*alt*-MAF-TBE) copolymer to serve as macroCTA for the successful synthesis of diblock terpolymers via RAFT was evidenced in a previous article.[49] Here, DMA and NIPAM were chosen as monomers for the synthesis of P(VAc-*alt*-MAF-TBE)-*b*-PDMA and P(VAc-*alt*-MAF-TBE)-*b*-PNIPAM diblock terpolymers, respectively (Table 1, entries 2-5). The successful syntheses of these diblock terpolymers were clearly evidenced by GPC and NMR spectroscopy.

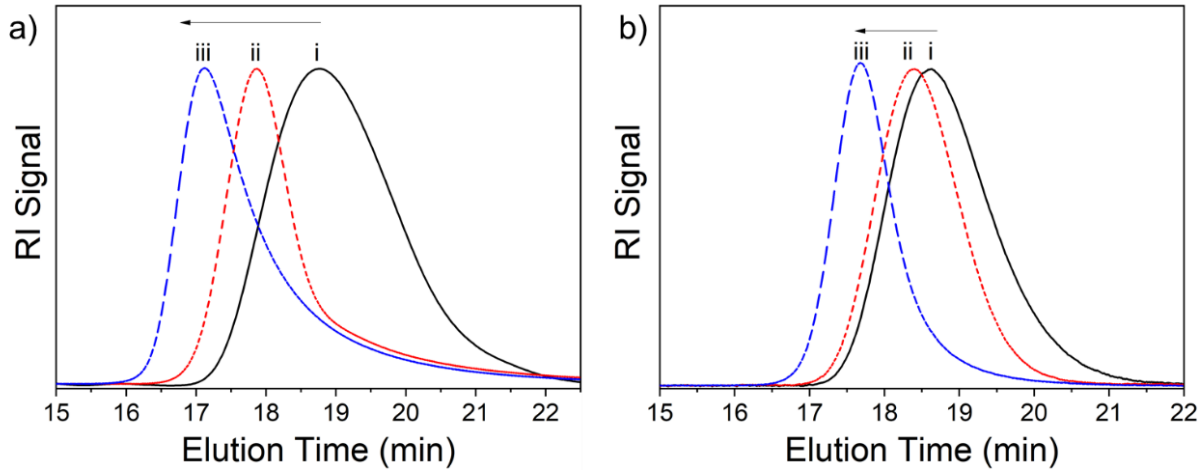

Figure 4. GPC chromatograms of the diblock terpolymers derived from P(VAc-*alt*-MAF-TBE) macroCTA. a) i (—) P(VAc-*alt*-MAF-TBE), ii (--) P(VAc-*alt*-MAF-TBE)-*b*-PDMA-1, iii (–––) P(VAc-*alt*-MAF-TBE)-*b*-PDMA-2. b) i (—) P(VAc-*alt*-MAF-TBE), ii (--) P(VAc-*alt*-MAF-TBE)-*b*-PNIPAM-1, iii (–––) P(VAc-*alt*-MAF-TBE)-*b*-PNIPAM-2.

Figures 4a and 4b display the GPC chromatograms of the P(VAc-*alt*-MAF-TBE)-*b*-PDMA and P(VAc-*alt*-MAF-TBE)-*b*-PNIPAM, respectively. The unimodal GPC traces of the diblock terpolymers shifted towards lower elution times indicating an increase in molar mass during the polymerizations of DMA or NIPAM. It is noteworthy to mention that the significant tailing of the chromatograms towards higher elution times (mainly visible in the case of P(VAc-*alt*-MAF-TBE)-*b*-PDMA) may be caused by residual macroCTA. This tailing also induces an increase in the dispersities of the diblock terpolymers. However, $Đ$ values remained relatively low (typically

below 1.45) and suggest an overall satisfactory level of control over the polymerization (Table 1).

^{1}H NMR spectroscopy provided additional information on the molar composition of the diblock terpolymers. Figure 5 depicts the ^{1}H NMR spectra of P(VAc-*alt*-MAF-TBE)-*b*-PDMA-1 (Figure 5a) and P(VAc-*alt*-MAF-TBE)-*b*-PNIPAM-1 diblock terpolymers (Figure 5b). Resonances assigned to both the DMA and NIPAM units were clearly observed. The presence of PDMA block is verified by the signal at 2.85 ppm assigned to the methyl groups (Figure 5a) while those at 1.13, 3.99 and 5.42 ppm in Figure 5b are attributed to -C<u>H</u>$(CH_3)_2$, -CH$(C\underline{H}_3)_2$ and -N<u>H</u>- groups, respectively, characteristic of the PNIPAM block.

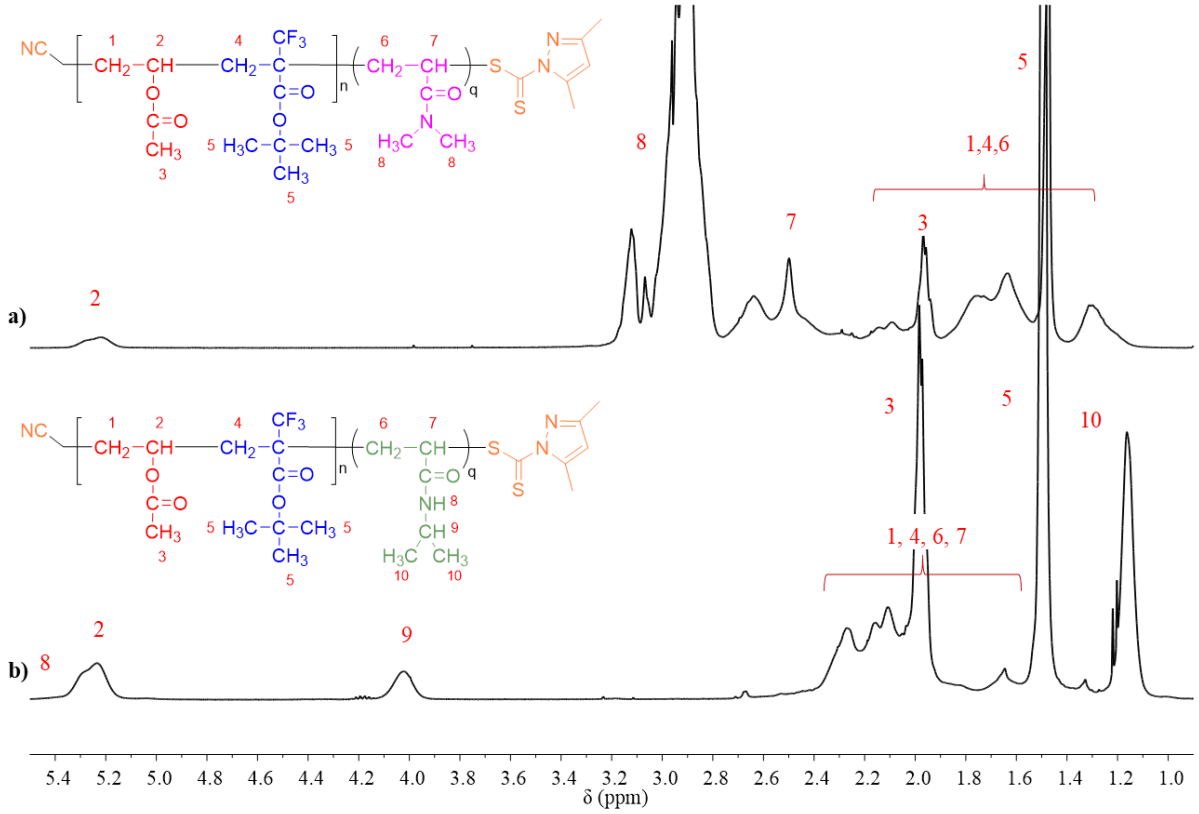

Figure 5. ^{1}H NMR spectra of: a) P(VAc-*alt*-MAF-TBE)-*b*-PDMA-1 and b) P(VAc-*alt*-MAF-TBE)-*b*-PNIPAM-1 diblock terpolymers recorded in $CDCl_3$.

Aqueous solution properties of P(VOH-*alt*-MAF)-*b*-PNIPAM diblock terpolymer as a function of solution pH

To study the aqueous solution properties of P(VOH-*alt*-MAF)-*b*-PNIPAM block copolymer, hydrolyses of the acetate groups of the VAc units into vinyl alcohol and of the *tert*-butyl ester groups of MAF-TBE units into carboxylic acid were carried out under the conditions used for the hydrolysis of P(VAc-*alt*-MAF-TBE) copolymer. The complete removal of both hydrophobic groups was evidenced by ^{13}C NMR spectroscopy (Figures 6a and 6b) showing the quantitative removal of acetate and *tert*-butyl ester groups by the vanishing of the resonances at 21.04 ppm (-$\underline{C}H_3$) and 27.73 ppm [-C($\underline{C}H_3$)$_3$], respectively.

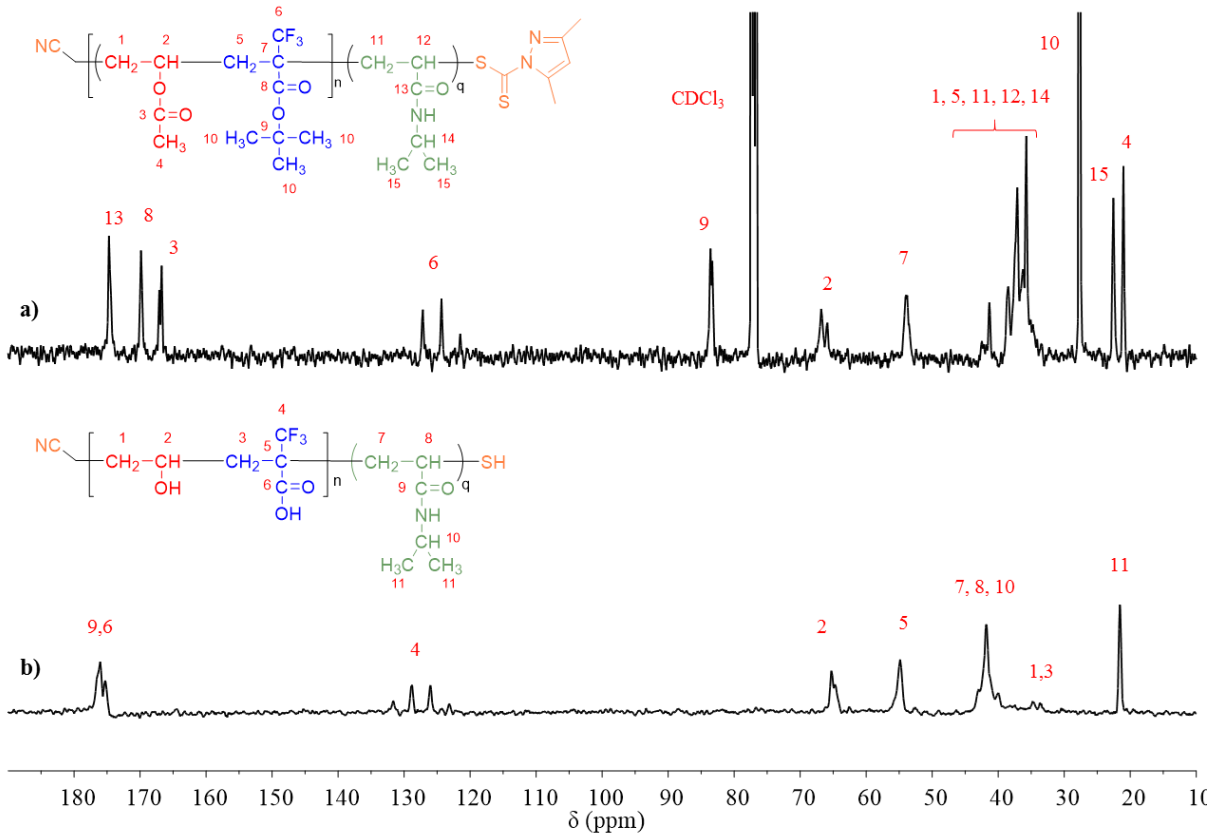

Figure 6. ^{13}C NMR spectra of: (a) P(VAc-*alt*-MAF-TBE)-*b*-PNIPAM-1 and (b) P(VOH-*alt*-MAF)-*b*-PNIPAM-1 diblock terpolymers recorded in $CDCl_3$ and D_2O, respectively.

Further evidence of hydrolysis of *tert*-butyl groups was evidenced by FTIR spectroscopy. The FTIR spectrum of P(VAc-*alt*-MAF-TBE)-*b*-PNIPAM-2 block terpolymer (Figure 1c) displays the characteristic absorption peaks of PNIPAM: at 2970 cm^{-1} C-H (asymmetric stretching), 2860 cm^{-1} C-H (symmetric stretching), 3305 cm^{-1} N-H (stretching), 1536 cm^{-1} C-N (stretching), 1459 - CH_3 (bending), and 1640 cm^{-1} (N-C=O) groups (stretching).[71] Removal of both hydrophobic groups resulted in the disappearance of peak at 1368 cm^{-1} assigned to *tert*-butyl groups of MAF-TBE, a slight downward shift of the C=O from 1743 cm^{-1} to 1592 cm^{-1} as well as the appearance of OH vibration band at 3100-3500 cm^{-1} (Figure 1d). At this point is should be pointed out that peaks of PNIPAM are still present after hydrolysis suggesting the structural integrity of the terpolymer. The simultaneous hydrolysis of both ester groups yielded the desired water-soluble pH- and thermo-responsive diblock terpolymer.

In addition, PNIPAM is a well-known hydrophilic polymer able to undergo a reversible lower critical solution temperature (LCST) phase transition above 32 ^{o}C.[72, 73] This results is a transition between a swollen hydrated state and a shrunk dehydrated state which further leads to aggregation of the polymer.[74] The aqueous solution properties of this dual-responsive polymer and the temperature-responsive properties of the P(VOH-*alt*-MAF)-*b*-PNIPAM diblock terpolymers as a function of temperature, solution pH and of PNIPAM content were assessed by UV/vis spectroscopy. The thermosensitivity was evidenced by monitoring the optical transmittance of a diblock terpolymer solution (1 wt%) as a function of solution pH, within the 20 - 80 °C temperature range.

Figure 7 exhibits the thermal response of P(VOH-*alt*-MAF)-*b*-PNIPAM-1 (37 % mol of PNIPAM) and P(VOH-*alt*-MAF)-*b*-PNIPAM-2 (61 % mol of PNIPAM) diblock terpolymers, at λ = 500 nm, for different pH values.

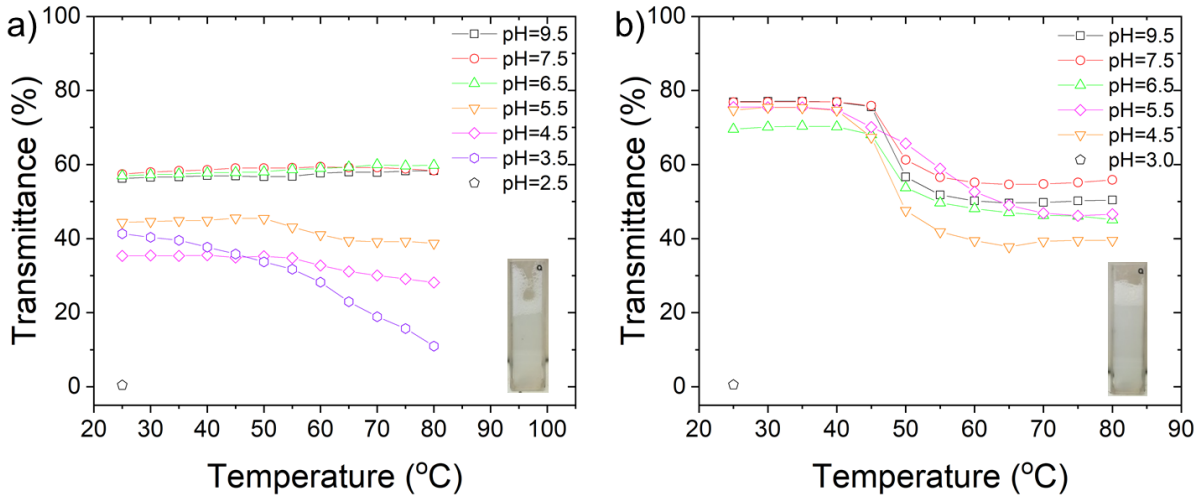

Figure 7. Optical transmittance at λ = 500 nm and c = 1 wt% of a) P(VOH-*alt*-MAF)-*b*-PNIPAM-1 (37 mol % of PNIPAM), and b) P(VOH-*alt*-MAF)-*b*-PNIPAM-2 (61 mol % of PNIPAM) diblock terpolymer solutions as a function of the pH and solution temperature. The insets represent pictures of vials at pH=2.5 (left) and pH = 3.0 (right) at room temperature.

The light transmittance profiles as a function of the solution temperature of the two diblock terpolymers exhibited different trends. It is worth noting that the initial transmittance in both figures is not 100%, suggesting that large aggregates had already formed at low temperature (vide infra). In the case of P(VOH-*alt*-MAF)-*b*-PNIPAM-1 diblock terpolymer from pH 9.5 to 6.5, the optical transmittance was independent of the temperature solution. As the solution pH was further reduced (from 5.5 to 3.5), the initial transmittance was gradually decreased. However, no macroscopic precipitation was clearly observed. At this pH regime, a small and progressive decrease of optical transmittance started around T = 50 °C and is likely due to the collapse of the PNIPAM sequences. This behavior became more pronounced at pH= 3.5 and started at lower temperature, around 35 °C (close to the LCST of PNIPAM). Finally, at pH 2.5, the solution became completely turbid at room temperature (Figure 7a, inset). These results may be explained as follows: In basic conditions, the electrostatic repulsive interactions derived from negatively charged MAF units prevent the terpolymer from phase separating. Therefore, there was no LCST found for the P(VOH-*alt*-MAF)-*b*-PNIPAM-1 diblock terpolymers at pH>6.5. This was only evidenced when the MAF units were progressively protonated and the entropy-

driven collapse of the PNIPAM block led to phase separation of the copolymer as illustrated by the decrease of the light transmittance from pH 5.5 to 3.5.

The thermoresponsive behavior of P(VOH-*alt*-MAF)-*b*-PNIPAM-2 followed a different trend (Figure 7b). Due to the higher PNIPAM content (61 mol %), the terpolymer chains were susceptible to changes of the temperature solution which were pH-independent. The transmittance decreases from ca. 45 °C over the entire range of pH tested (from pH 9.5 to 4.5). The LCST of PNIPAM seemed to be shifted towards higher temperature (45 °C instead of 32 °C) probably on account of negatively charged MAF groups. However, at pH= 3.0 and T = 25 °C the system changed from transparency to opacity due to the aggregation of the polymer chains (Figure 7b, inset). This phenomenon is somewhat surprising as this diblock terpolymer was expected to be more hydrophilic and thus soluble over the entire pH range due to the higher PNIPAM content. We strongly believe that as in the case of P(VOH-*alt*-MAF)-*b*-PNIPAM-1, the hydrophobic interactions between the trifluoromethyl groups become dominant at low pH, even at temperatures below the LCST of PNIPAM, leading to the macroscopic precipitation of the terpolymers. Analogous phenomena were found for dual responsive poly(2-(dimethylamino)ethyl methacrylate)-*b*-poly(acrylic acid) (PDMAEMA-*b*-PAA) diblock copolymers.[75] Importantly, all these macroscopic phase transitions were reversible; the turbid terpolymer solution turned transparent under alkaline pH conditions at ambient temperature. These results demonstrate that these fluorinated diblock terpolymers exhibit both pH and thermal responsive properties and that their LCST is affected by their compositions and the solution pH.

Then, the aqueous solution properties of the terpolymers were investigated by DLS. Figure 8 exhibits the average hydrodynamic diameters (D_h) of PNIPAM block terpolymers as a function of the solution pH at 25 °C. At a pH ranging between 10 and 4, two main populations were observed. The most abundant population with D_h = 11 ± 1 nm and D_h = 17 ± 4 nm for P(VOH-*alt*-MAF)-*b*-PNIPAM-1 and P(VOH-*alt*-MAF)-*b*-PNIPAM-2, respectively was attributed to single terpolymer chains (unimers), while the second population with D_h = 195 ± 30 nm and D_h = 625 ± 140 nm for P(VOH-*alt*-MAF)-*b*-PNIPAM-1 and P(VOH-*alt*-MAF)-*b*-PNIPAM-2, respectively were assigned to aggregates. The presence of large aggregates in both polymer solutions rationalizes the rather low transmittance observed at room temperature during UV/vis studies (Figures 7a, 7b). As the solution pH was further decreased (pH ≤ 4), a unique population

was observed indicating the formation of large aggregates as it was also evidenced by UV/vis spectroscopy in the same pH regime.

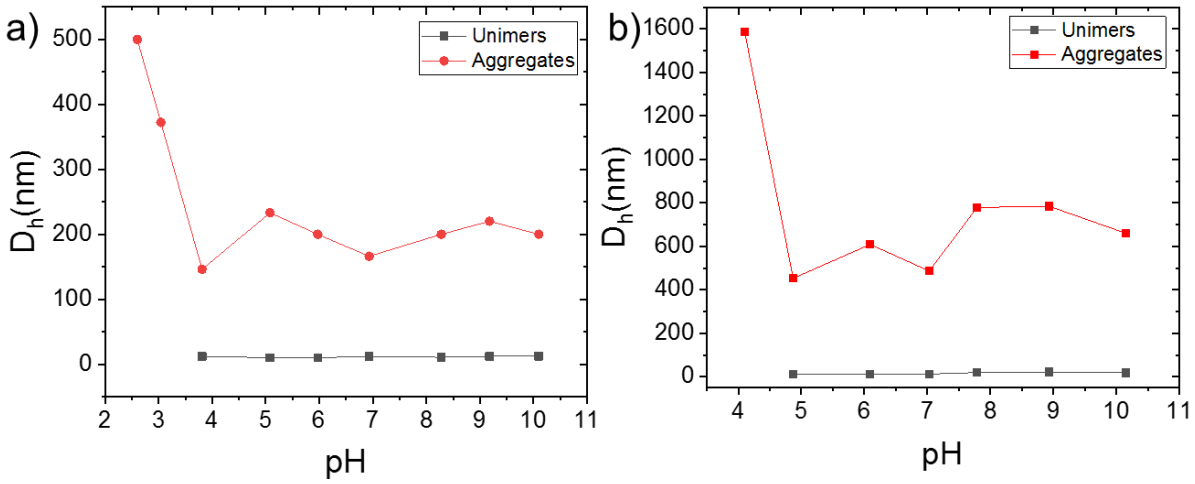

Figure 8. Variation of the hydrodynamic diameter of a 0.1 wt % P(VOH-*alt*-MAF)-*b*-PNIPAM-1 (a) and P(VOH-*alt*-MAF)-*b*-PNIPAM-2 (b) copolymer solution in water as a function of the solution pH at 25 ^{o}C.

Solution self-assembly of P(VAc-*alt*-MAF-TBE)-*b*-PDMA and P(VAc-*alt*-MAF-TBE)-*b*-PNIPAM diblock terpolymers: effect of the block length

Structures obtained by self-assembly of amphiphilic block copolymers are often dictated by their hydrophobic/hydrophilic balance.[76] Both P(VAc-*alt*-MAF-TBE)-*b*-PDMA and P(VAc-*alt*-MAF-TBE)-*b*-PNIPAM are amphiphilic diblock terpolymers which consist of a hydrophobic alternating P(VAc-*alt*-MAF-TBE) sequence and a hydrophilic PDMA or PNIPAM block.[47] The influence of the length of the hydrophilic segment on the aggregation behavior of these amphiphilic copolymers was studied by transmission electron microscopy (TEM) (Figure 9).

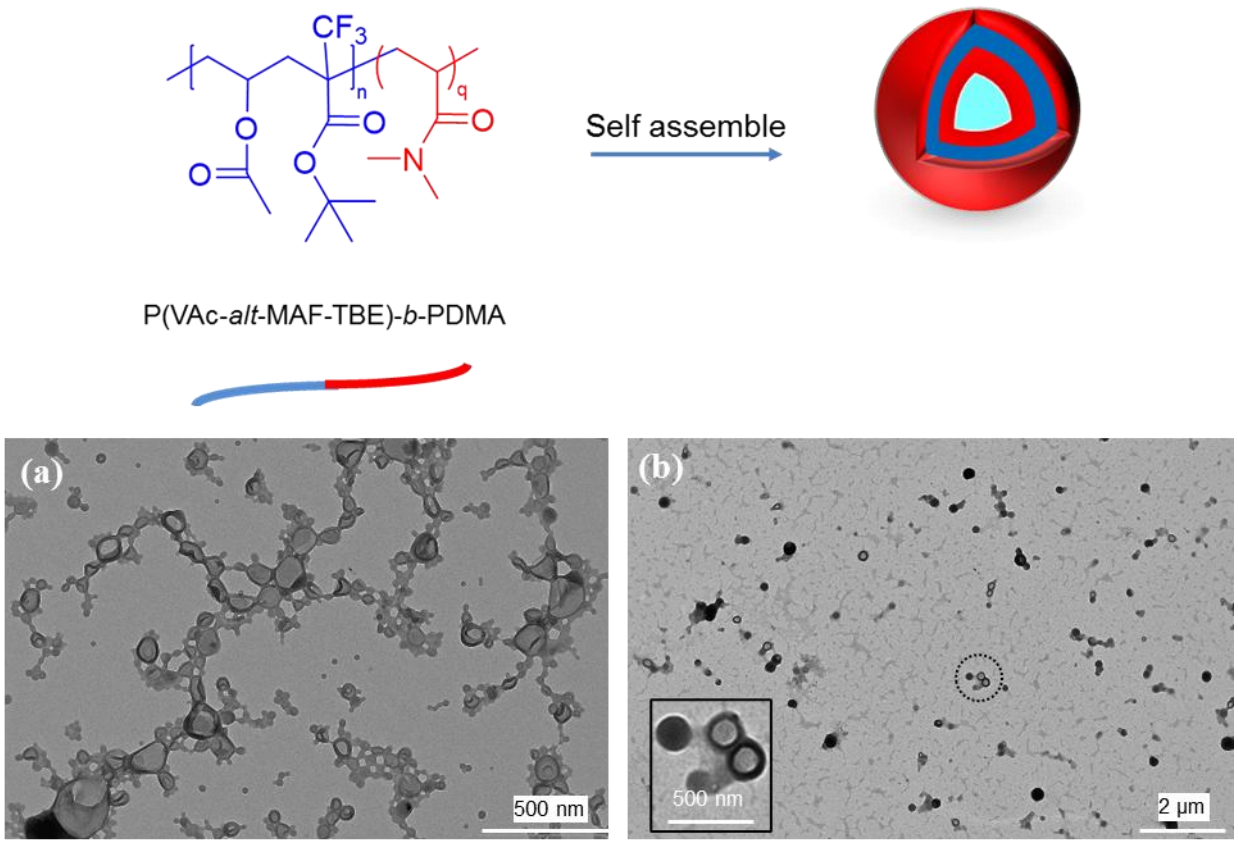

Figure 9. Schematic illustration depicting the self-assembly of P(VAc-*alt*-MAF-TBE)-*b*-PDMA diblock terpolymers into vesicles in water. TEM micrographs of self-assembled P(VAc-*alt*-MAF-TBE)-*b*-PDMA-1 and P(VAc-*alt*-MAF-TBE)-*b*-PDMA-2 diblock terpolymers (a and b, respectively) at pH=7.0 and 25 °C. The insets are zoomed area of the dotted circle.

Polydispersed interconnected vesicular structures with an average diameter equal to D = 146 ± 69 nm (Figure 9a) were observed for P(VAc-*alt*-MAF-TBE)-*b*-PDMA-1 diblock terpolymers. The dark parts located at the peripheral layer of the vesicles are attributed to the electron-rich fluorine atoms.[77, 78] Increasing the hydrophilic DMA block from 52 to 79 mol %, increased the average diameter of the vesicles to D = 260 ± 99 nm (Figure 9b). The average hydrodynamic diameter of the vesicles was also calculated by DLS and was found to be D_h = 160 ± 98 nm for P(VAc-*alt*-MAF-TBE)-*b*-PDMA-1 and D_h = 419 ± 318 nm for P(VAc-*alt*-MAF-TBE)-*b*-PDMA-2 diblock terpolymers (Figures S9a, S9b).

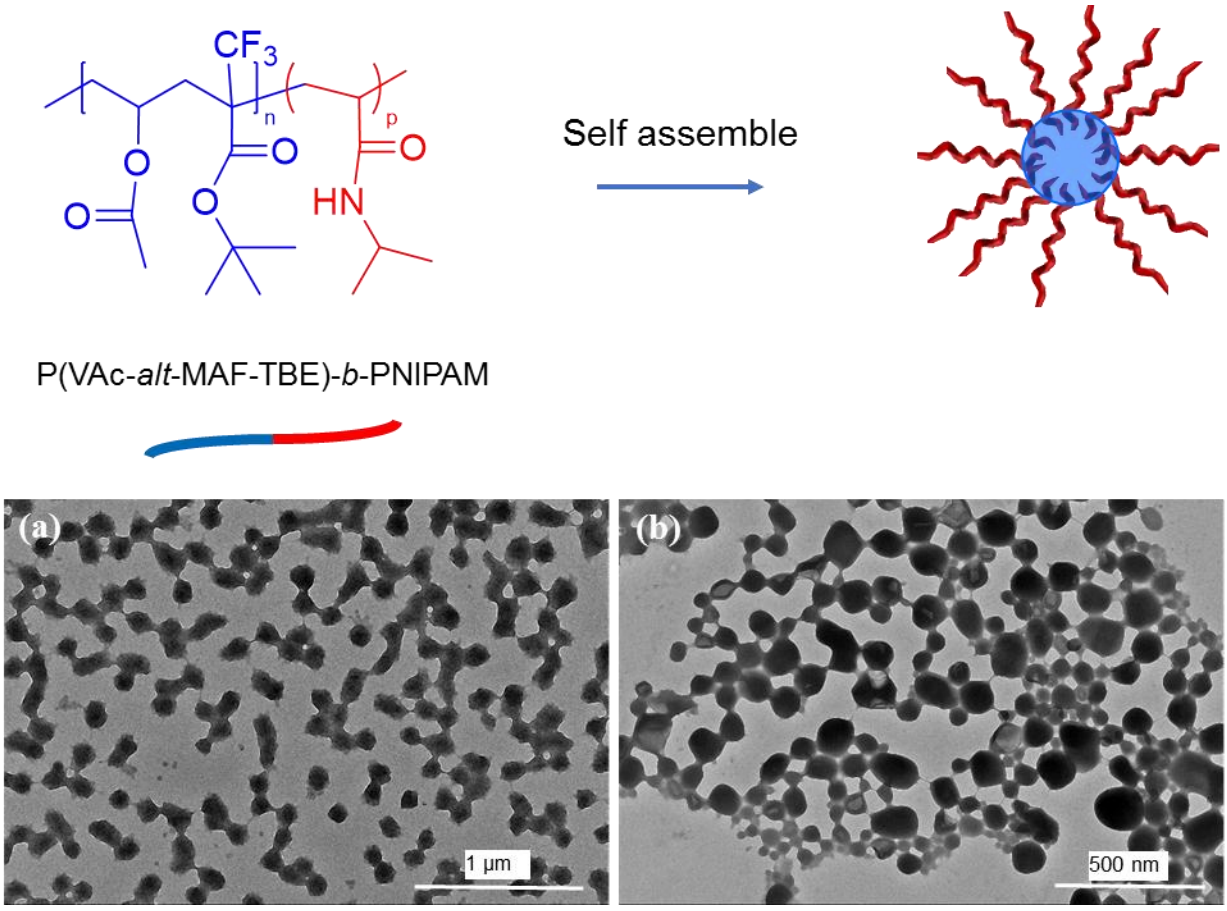

Figure 10. Schematic illustration depicting the self-assembly of P(VAc-*alt*-MAF-TBE)-*b*-PNIPAM diblock terpolymers into micelles in water. TEM micrographs of self-assembled P(VAc-*alt*-MAF-TBE)-*b*-PNIPAM-1 and P(VAc-*alt*-MAF-TBE)-*b*-PNIPAM-2 diblock terpolymers (a and b, respectively) at pH=7.0 and 25 °C.

On the contrary, PNIPAM based terpolymers self-assembled into spherical micelles in water where the dark micelle core region correspond to CF_3 domains,[77, 78] while the hydrophilic PNIPAM block extends in solution to form the micelle corona, as it is observed by TEM analysis (Figures 10a, 10b). An average size of D = 130 ± 20 nm was measured for P(VAc-*alt*-MAF-TBE)-*b*-PNIPAM-1 terpolymers while the average diameter was increased to D = 300 ± 90 nm for the diblock terpolymers featuring longer PNIPAM blocks (61 mol %). The respective average hydrodynamic diameters of the micellar structures were found to be D_h = 137 ± 66 nm and D_h = 383 ± 250 nm (Figures S9c, S9d). Average diameters calculated by TEM and DLS were in a

relatively good agreement further confirming that these micelles can remain stable and readily dispersed in aqueous solution.

Solution self-assembly P(VOH-*alt*-MAF)-*b*-PNIPAM block terpolymers: effect of pH

Since the hydrolyzed diblock terpolymer, P(VOH-*alt*-MAF)-*b*-PNIPAM, was found to be pH-sensitive, the effect of pH on its self-assembly was investigated. Figure 11 displays the TEM images of both P(VOH-*alt*-MAF)-*b*-PNIPAM-1 terpolymers at pH 9.5 and 3.5 at 25 °C.

At pH 9.5, random sized vesicular structures with average size D = 430 ± 220 nm were observed for P(VOH-*alt*-MAF)-*b*-PNIPAM-1 diblock terpolymer (Figure 11a). Interestingly, decreasing the solution pH solution of these vesicular dispersions from solution from pH 9.5 to 3.5 led to vesicle-to-sphere transition (Figure 11b). These spherical nanoparticles with an average diameter of D = 340 ± 220 nm had crossed dark lines in their centers which are attributed to fluorine moieties. Presumably, the protonation of carboxylate groups caused an increase of the hydrophobicity of the P(VOH-*alt*-MAF) block which led to a change in terpolymer morphology. Diblock terpolymers featuring longer PNIPAM blocks (61 mol %) at pH=9.5, did not exhibit any clear self-assembled structures, while at pH= 3.5 polydispersed vesicular structures were formed (Figure S10).

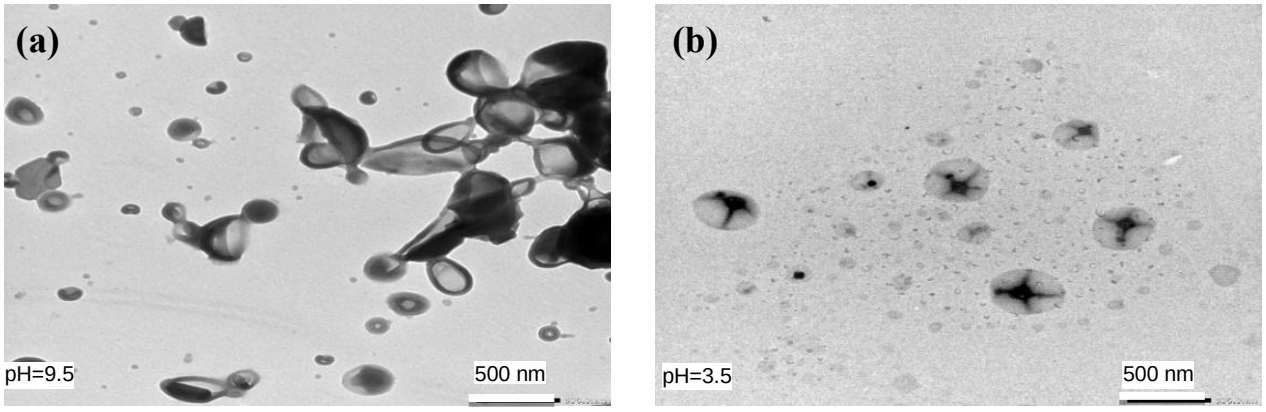

Figure 11. TEM micrographs of self-assembled P(VOH-*alt*-MAF)-*b*-PNIPAM-1 at pH=9.5 (a) and pH=3.5 (b).

Conclusions

This article explores the impact of trifluoromethyl groups on the aqueous solution properties of dual-responsive terpolymers. Using sequential RAFT polymerization, well-defined P(VAc-*alt*-MAF-TBE)-*b*-PNIPAM and P(VAc-*alt*-MAF-TBE)-*b*-PDMA diblock terpolymers were prepared, displaying relatively narrow dispersities ($Đ$=1.21-1.45). The complete hydrolysis of the ester groups in the P(VAc-*alt*-MAF-TBE) macroCTA was verified by ^{13}C NMR and FTIR spectroscopy. The resulting copolymer was water-soluble in alkaline media owing to the ionization of the carboxylate groups. The dilute aqueous solution properties were studied in some detail. Titrations and zeta potential measurements showed that the copolymer underwent a phase transition under acidic conditions (pH<3). This was likely due to the presence of trifluoromethyl groups which induced hydrophobic interactions able to overcome the strong electrostatic interactions and drive in turn to macroscopic phase separation. In addition, the synergetic effect of two external stimuli, pH and temperature, in the P(VOH-*alt*-MAF)-*b*-PNIPAM terpolymers of different PNIPAM block lengths was also studied by turbidity measurements. The results indicated that the phase transition and responsive behavior of the diblock terpolymers were affected by both the solution pH and the composition of the copolymers. Diblock terpolymers with higher PNIPAM content demonstrated a sharper transition behavior at LCST ca. 50 ^{o}C from pH 9.5 to 4.5 while at lower pH, a macroscopic separation was observed. This suggests that the diblock terpolymer underwent a hydrophilic-hydrophobic transition driven by the progressive protonation of the carboxylate groups of MAF units. TEM studies revealed that the P(VAc-*alt*-MAF-TBE)-*b*-PDMA and P(VAc-*alt*-MAF-TBE)-*b*-PNIPAM diblock terpolymers self-assembled to vesicular and micellar structures, respectively. The supramolecular organization of P(VOH-*alt*-MAF)-*b*-PNIPAM terpolymers was affected by the electrostatic interaction between negatively charged carboxylate groups and hydrophobic interactions of fluorine groups. This study indicated that the present diblock terpolymers can be used as paradigm for the preparation to a multitude of new "smart" functional fluorine containing materials which can been employed for advanced biomedical applications.

Notes

The authors declare no competing financial interest.

Acknowledgements

This work was supported by a consolidator fellowship from the European Research Council ERC (SENSOILS-647857) and from the French National Agency (ANR grant FLUPOL; contract No. ANR-14-CE07-0012). The authors thank Tosoh Fine Chemical Corporation, Shunan, Japan for supplying MAF-TBE and Dr Mona Semsarilar and Dr Enrique Folgado for their scientific contributions with Transmission Electron Microscopy pictures.

References

1. M. Wei, Y. Gao, X. Li and M. J. Serpe, *Polymer Chemistry*, 2017, **8**, 127-143.
2. O. E. Philippova, D. Hourdet, R. Audebert and A. R. Khokhlov, *Macromolecules*, 1997, **30**, 8278-8285.
3. S. Y. Park and Y. H. Bae, *Macromolecular Rapid Communications*, 1999, **20**, 269-273.
4. J. E. Chung, M. Yokoyama and T. Okano, *Journal of Controlled Release*, 2000, **65**, 93-103.
5. M. C. Chiappelli and R. C. Hayward, *Advanced Materials*, 2012, **24**, 6100-6104.
6. F. D. Jochum and P. Theato, *Chemical Communications*, 2010, **46**, 6717-6719.
7. V. K. Kotharangannagari, A. Sánchez-Ferrer, J. Ruokolainen and R. Mezzenga, *Macromolecules*, 2011, **44**, 4569-4573.
8. J. Babin, J. Rodriguez-Hernandez, S. Lecommandoux, H. A. Klok and M. F. Achard, *Faraday Discussions*, 2005, **128**, 179-192.
9. L. Zhang, T. L. U. Nguyen, J. Bernard, T. P. Davis, C. Barner-Kowollik and M. H. Stenzel, *Biomacromolecules*, 2007, **8**, 2890-2901.
10. D. A. Davis, A. Hamilton, J. Yang, L. D. Cremar, D. Van Gough, S. L. Potisek, M. T. Ong, P. V. Braun, T. J. Martínez, S. R. White, J. S. Moore and N. R. Sottos, *Nature*, 2009, **459**, 68.
11. H. Zhang, Y. Chen, Y. Lin, X. Fang, Y. Xu, Y. Ruan and W. Weng, *Macromolecules*, 2014, **47**, 6783-6790.
12. Y. Zhang, S. Chen, M. Pang and W. Zhang, *Polymer Chemistry*, 2016, **7**, 6880-6884.
13. Q.-S. Tong, W. Xu, Q.-Y. Huang, Y.-R. Zhang, X.-X. Shi, H. Huang, H.-J. Li, J.-Z. Du and J. Wang, *Polymer Chemistry*, 2019, **10**, 656-662.
14. P. G. Falireas and M. Vamvakaki, *Macromolecules*, 2018, **51**, 6848-6858.

15. J. G. Hardy, E. Larrañeta, R. F. Donnelly, N. McGoldrick, K. Migalska, M. T. C. McCrudden, N. J. Irwin, L. Donnelly and C. P. McCoy, *Molecular Pharmaceutics*, 2016, **13**, 907-914.
16. J. Xu and S. Liu, *Soft Matter*, 2008, **4**, 1745-1749.
17. M. Toma, U. Jonas, A. Mateescu, W. Knoll and J. Dostalek, *The Journal of Physical Chemistry C*, 2013, **117**, 11705-11712.
18. S. W. Hong, D. Y. Kim, J. U. Lee and W. H. Jo, *Macromolecules*, 2009, **42**, 2756-2761.
19. S. Maji, B. Cesur, Z. Zhang, B. G. De Geest and R. Hoogenboom, *Polymer Chemistry*, 2016, **7**, 1705-1710.
20. M. Motornov, R. Sheparovych, R. Lupitskyy, E. MacWilliams, O. Hoy, I. Luzinov and S. Minko, *Advanced Functional Materials*, 2007, **17**, 2307-2314.
21. B. P. Binks, R. Murakami, S. P. Armes and S. Fujii, *Angewandte Chemie International Edition*, 2005, **44**, 4795-4798.
22. H. S. Sundaram, Y. Cho, M. D. Dimitriou, J. A. Finlay, G. Cone, S. Williams, D. Handlin, J. Gatto, M. E. Callow, J. A. Callow, E. J. Kramer and C. K. Ober, *ACS Applied Materials & Interfaces*, 2011, **3**, 3366-3374.
23. Z. Cui, E. Drioli and Y. M. Lee, *Prog. Polym. Sci.*, 2013, **39**, 164-198.
24. J. E. Hensley and J. D. Way, *Chemistry of Materials*, 2007, **19**, 4576-4584.
25. B. Ameduri and B. Boutevin, in *Well-Architectured Fluoropolymers: Synthesis, Properties and Applications*, Elsevier Science, Amsterdam, 2004, DOI: https://doi.org/10.1016/B978-008044388-1/50010-8, pp. 1-99.
26. J. Scheirs, *Modern fluoropolymers : high performance polymers for diverse applications*, Wiley, Chichester, 1997.
27. D. Smith, S. Iacono and S. S. Iyer, *Handbook of Fluoropolymer Science and Technology*, Wiley, New York, 2014.
28. B. Ameduri and H. Sawada, *Fluorinated Polymers : Volume 2: Applications*, RSC, Oxford, 2016.
29. V. F. Cardoso, D. M. Correia, C. Ribeiro, M. M. Fernandes and S. Lanceros-Méndez, *Polymers*, 2018, **10**, 161.
30. C. A. Gough, D. A. Pearlman and P. Kollman, *The Journal of Chemical Physics*, 1993, **99**, 9103-9110.
31. P. Selvam, R. P. S. Peguin, U. Chokshi and S. R. P. da Rocha, *Langmuir*, 2006, **22**, 8675-8683.
32. C. Porsch, Y. Zhang, Å. Östlund, P. Damberg, C. Ducani, E. Malmström and A. M. Nyström, *Particle & Particle Systems Characterization*, 2013, **30**, 381-390.
33. M. Wang, H. Liu, L. Li and Y. Cheng, *Nature Communications*, 2014, **5**, 3053.

34. D. Churchley, G. Rees, E. Barbu, T. Nevell and J. Tsibouklis, *International journal of pharmaceutics*, 2008, **352**, 44-49.
35. P. Zhu, W. Meng and Y. Huang, *RSC Advances*, 2017, **7**, 3179-3189.
36. Z. Wang and H. Zuilhof, *Langmuir*, 2016, **32**, 6571-6581.
37. J. G. Riess and M. P. Krafft, *Biomaterials*, 1998, **19**, 1529-1539.
38. J. Singh and K. K. Agrawal, *Journal of Macromolecular Science, Part C*, 1992, **32**, 521-534.
39. X. Zhao, Y. Su, W. Chen, J. Peng and Z. Jiang, *Journal of Membrane Science*, 2011, **382**, 222-230.
40. Z.-C. Chen, B.-C. Zhu, J.-J. Li, Y.-N. Zhou and Z.-H. Luo, *Journal of Polymer Science Part A: Polymer Chemistry*, 2016, **54**, 3868-3877.
41. F. Zuppardi, F. R. Chiacchio, R. Sammarco, M. Malinconico, G. Gomez d'Ayala and P. Cerruti, *Polymer*, 2017, **112**, 169-179.
42. G. Liu, X. Li, S. Xiong, L. Li, P. K. Chu, S. Wu and Z. Xu, *Journal of Fluorine Chemistry*, 2012, **135**, 75-82.
43. J. M. Bak, K.-B. Kim, J.-E. Lee, Y. Park, S. S. Yoon, H. M. Jeong and H.-i. Lee, *Polymer Chemistry*, 2013, **4**, 2219-2223.
44. J. M. Bak and H.-i. Lee, *Journal of Polymer Science Part A: Polymer Chemistry*, 2013, **51**, 1976-1982.
45. Y.-N. Zhou, J.-J. Li, Q. Zhang and Z.-H. Luo, *Langmuir*, 2014, **2014 v.30 no.41**, pp. 12236-12242.
46. C. Liu, J. He, Q. Zhao, M. Zhang and P. Ni, *Journal of Polymer Science Part A: Polymer Chemistry*, 2009, **47**, 2702-2712.
47. A. J. Convertine, B. S. Lokitz, Y. Vasileva, L. J. Myrick, C. W. Scales, A. B. Lowe and C. L. McCormick, *Macromolecules*, 2006, **39**, 1724-1730.
48. J. Gardiner, I. Martinez-Botella, J. Tsanaktsidis and G. Moad, *Polymer Chemistry*, 2016, **7**, 481-492.
49. S. Banerjee, M. Guerre, B. Améduri and V. Ladmiral, *Polymer Chemistry*, 2018, **9**, 3511-3521.
50. M. Shirai, S. Takashiba and M. Tsunooka, *Journal of Photopolymer Science and Technology*, 2003, **16**, 545-548.
51. H. Ito, H. D. Truong, M. Okazaki and R. A. DiPietro, *Journal of Photopolymer Science and Technology*, 2003, **16**, 523-536.
52. V. R. Vohra, K. Douki, Y. J. Kwark, X. Q. Liu, C. K. Ober, Y. C. Bae, W. Conley, D. Miller and P. Zimmerman, in *Advances in Resist Technology and Processing Xix, Pts 1 and 2*, ed. T. H. Fedynyshyn, 2002, vol. 4690, pp. 84-93.
53. C. K. Ober, K. Douki, V. R. Vohra, Y. J. Kwark, X. Q. Liu, W. Conley, D. Miller and P. Zimmerman, *Journal of Photopolymer Science and Technology*, 2002, **15**, 603-611.

54. Y. Patil and B. Ameduri, *Progress in Polymer Science*, 2013, **38**, 703-739.
55. H. Ito, B. Giese and R. Engelbrecht, *Macromolecules*, 1984, **17**, 2204-2205.
56. K. T. McElroy, S. T. Purrington, C. L. Bumgardner and J. P. Burgess, *Journal of Fluorine Chemistry*, 1999, **95**, 117-120.
57. T. Narita, T. Hagiwara, H. Hamana and T. Nara, *Die Makromolekulare Chemie, Rapid Communications*, 1985, **6**, 301-304.
58. T. Narita, T. Hagiwara, H. Hamana and S. Maesaka, *Polymer Journal*, 1988, **20**, 519.
59. Y. Patil, A. Alaaeddine, T. Ono and B. Ameduri, *Macromolecules*, 2013, **46**, 3092-3106.
60. Y. Patil and B. Ameduri, *Polymer Chemistry*, 2013, **4**, 2783-2799.
61. S. Banerjee, T. Soulestin, Y. Patil, V. Ladmiral and B. Ameduri, *Polymer Chemistry*, 2016, **7**, 4004-4015.
62. P. G. Falireas, M. Wehbi, A. Alaaeddine and B. Améduri, *Polymer Chemistry*, 2018, **9**, 3754-3761.
63. S. Banerjee, V. Ladmiral, A. Debuigne, C. Detrembleur, S. M. W. Rahaman, R. Poli and B. Ameduri, *Macromolecular Rapid Communications*, 2017, **38**, 1700203.
64. S. Banerjee, V. Ladmiral, C. Totée and B. Améduri, *European Polymer Journal*, 2018, **104**, 164-169.
65. E. Poggi, C. Guerlain, A. Debuigne, C. Detrembleur, D. Gigmes, S. Hoeppener, U. S. Schubert, C.-A. Fustin and J.-F. Gohy, *European Polymer Journal*, 2015, **62**, 418-425.
66. S. G. Boyes, B. Akgun, W. J. Brittain and M. D. Foster, *Macromolecules*, 2003, **36**, 9539-9548.
67. A. Debuigne, J. Warnant, R. Jérôme, I. Voets, A. de Keizer, M. A. Cohen Stuart and C. Detrembleur, *Macromolecules*, 2008, **41**, 2353-2360.
68. M. Guerre, J. Schmidt, Y. Talmon, B. Améduri and V. Ladmiral, *Polymer Chemistry*, 2017, **8**, 1125-1128.
69. E. V. Piletska, A. R. Guerreiro, M. Romero-Guerra, I. Chianella, A. P. F. Turner and S. A. Piletsky, *Analytica Chimica Acta*, 2008, **607**, 54-60.
70. E. P. C. Lai and S. Y. Feng, *Microchemical Journal*, 2003, **75**, 159-168.
71. Y. Katsumoto, T. Tanaka, H. Sato and Y. Ozaki, *The Journal of Physical Chemistry A*, 2002, **106**, 3429-3435.
72. H. G. Schild, *Progress in Polymer Science*, 1992, **17**, 163-249.
73. M. Shibayama, T. Norisuye and S. Nomura, *Macromolecules*, 1996, **29**, 8746-8750.
74. Y. Cao, X. X. Zhu, J. Luo and H. Liu, *Macromolecules*, 2007, **40**, 6481-6488.

75. X. Han, X. Zhang, H. Zhu, Q. Yin, H. Liu and Y. Hu, *Langmuir*, 2013, **29**, 1024-1034.
76. Y. Mai and A. Eisenberg, *Chemical Society Reviews*, 2012, **41**, 5969-5985.
77. Z. Li, E. Kesselman, Y. Talmon, M. A. Hillmyer and T. P. Lodge, *Science*, 2004, **306**, 98-101.
78. H. S. Hwang, H. J. Kim, Y. T. Jeong, Y.-S. Gal and K. T. Lim, *Macromolecules*, 2004, **37**, 9821-9825.

GRAPHICAL ABSTRACT

For Table of Contents Use only